Hydrogen fluoride phase behavior and molecular structure: *Ab initio* derived potential models

Scott J. Wierzchowski and David A. Kofke[a)]
Department of Chemical Engineering, University at Buffalo, The State University of New York, Buffalo, New York 14260-4200

(Received 22 April 2003; accepted 27 June 2003)

Several variations of *ab initio* based molecular models for hydrogen fluoride (HF) are examined by Monte Carlo molecular simulation to determine their bulk-phase properties. The models are taken from the literature, and represent fits of functional forms to the potential energy surface of the HF dimer as given by *ab initio* computational chemistry calculations. For one of these models, we examine three variations for bulk-phase modeling. In particular, we consider first the effect of including versus neglecting an Ewald sum for the long-range dipole–dipole interactions; second, we examine a modification of the form for the short range repulsive region of the potential; and third, we add three-body contributions to the energy via an available 12-dimensional potential for the trimer, again representing a fit to *ab initio* energy calculations. The simulations examine the density (via isothermal–isobaric simulation) and radial distribution function (via canonical–ensemble simulations) each at two state points where corresponding experimental data are available. We also examine vapor–liquid coexistence properties, considering the saturation densities, heat of vaporization, and vapor pressure from 225 K to states approaching (but not closely) each model's critical point. Inclusion of the three-body energy is the only variation that has any beneficial effect on the radial distribution function as compared to experiment, and this variation also gives good results for the vapor pressure, and significantly raises the critical point toward the experimental value. However this model also grossly overestimates the liquid-phase coexistence density. In almost all regards none of the models or variations can be considered to give a satisfactory representation of the bulk-phase behavior. Improvements to the models require more careful attention to the balance between repulsive and attractive pair interactions at short range. © *2003 American Institute of Physics.* [DOI: 10.1063/1.1602068]

I. INTRODUCTION

Molecular simulation is being increasingly viewed as a viable tool to supplement or in some cases replace experimental investigations. This is a desirable goal because for many systems it is less expensive and perhaps less hazardous to ''measure'' properties via simulation rather than experiment. Of course, the practice of replacing experiment with simulation has important caveats, not the least of which is the significant likelihood of obtaining incorrect results. The success of simulation in reproducing experimental measurements is unavoidably linked to the potential energy surface used to model the intermolecular interactions. To ever serve as a complete replacement for experiment, simulation must be able to do more than fit and provide a basis to extrapolate existing data (although this practice too is useful in itself). Molecular simulation as a truly predictive tool requires that a potential surface be available from first-principles considerations, or at least be able to be assembled from a set of pre-existing potentials describing interactions between functional groups. Using the latter approach, the properties of many relatively simple molecular systems can and have been predicted quite well in comparison to experiment.[1]

Associating fluids such as water, ammonia, hydrogen fluoride (HF) and acetic acid are particularly challenging for predictive calculations. The properties of these systems are greatly impacted by the hydrogen-bonding structures and networks that they form, and these features can be delicately dependent upon details of the intermolecular potential. Not coincidentally such systems are most interesting from a practical and scientific point of view, so potential energy surfaces for associating molecules have been developed for them via a variety of methodologies, most involving a fit to experimental data for the bulk phase properties.

The Car–Parrinello molecular dynamics method[2] presents a means to apply *ab initio* potential energy calculations simultaneously with a molecular simulation, using the *ab initio* generated forces and energies to guide the evolution of the simulation. This method has limitations, and in particular the use of plane-wave basis makes it weak in characterizing dispersion interactions. However, it has been used to good effect in strongly hydrogen-bonding systems,[3] and HF in particular,[4] where dispersion is less important. Nevertheless this application has been performed for relatively small liquid-phase systems only, and no attempt has been made, for example, to compute vapor-liquid coexistence with this method.

Car–Parrinello notwithstanding, it is still not generally

a)Author to whom correspondence should be addressed; electronic mail: kofke@buffalo.edu

feasible to apply *ab initio* calculations to characterize potential energy surfaces on-the-fly during a molecular simulation. Consequently, first-principles methods must take an approach in which empirical potential-energy surfaces are obtained by fitting functional forms to the results of *ab initio* calculations. This approach has gained interest through recent studies in which it has demonstrated some success for a variety of molecular species.[5–7] Advantages in this approach are also realized when one deals with mixtures. First-principles techniques eliminate the need for treating cross interactions with such approaches as Lorentz–Berthelot mixing rules. Further, the advent of faster computing facilities and availability of extensive and user-friendly *ab initio* packages makes such techniques a viable means to predict interaction energies.

Although some successes exist for *ab initio* derived potentials applied to calculating fluid properties of polar molecules,[8,9] the molecule HF presents a problem even for potentials fit to high levels of theory.[7,10] In particular, the phase equilibrium properties have not been estimated well[7,11] using these models. The failure is characterized by the overestimation of liquid densities on the vapor–liquid coexistence line. The potential models used in such studies are mainly two-body forms based on dimer calculations[12] which one could expect to fare poorly in characterizing condensed-phase properties. One might anticipate that the understanding and inclusion of multibody effects in these models would be a reasonable step toward remedying this problem. Indeed it has been seen that the application of three body terms to the simulations of water has improved liquid phase structures.[9,13] Quack *et al.*[14] among others[15,16] give evidence and motivation for including higher order terms for HF modeling. Further they reveal evidence that just three-body interactions might be sufficient to obtain good results.[14]

Simulation necessarily uses potential truncation to accelerate ensemble sampling. To correct this approximation, non-Coulombic long-range interactions are accounted for by integration over a set cutoff outward, assuming no pair correlation.[17,18] Accounting for long-range electrostatic effects is more difficult, and typically involves Ewald summations, reaction field, or other more sophisticated techniques.[19,20] However the computational expense and programming effort in many cases leads these corrections to be neglected entirely. One way to justify this choice is to point out that the pair potential is an effective potential, not the true one, and the process of fitting to experimental data accounts for, among other things, errors due to the electrostatic truncation. This argument cannot be made if the potential is formulated from *ab initio* calculations, so it is worthwhile to consider the effect of neglecting or correcting for neglect of long-range electrostatics on bulk-phase properties modeled by these potentials.

Another concern is connected to the treatment of short-range repulsive interactions, which may be handled poorly by means of a fitted *ab initio* technique. It has already been shown that the intermolecular Coulomb part at short ranges affects the property calculations for some point-charge models.[21] For potential models that include Lennard-Jones or Exp-6, short-range repulsion in HF[16,22] is properly handled when fitting parameters to bulk-phase experimental data. Klein *et al.*[23] noted the difficulty in calculating liquid properties exclusively from *ab initio* data. They developed a potential model that considers both *ab initio* data and experimental fluid properties. The model included Born–Mayer repulsion between hydrogen atoms (a repulsion that many models deal with only through charge interactions). Further, *ab initio* calculations typically underemphasize higher energetic (repulsive) regions and focus on configurations where hydrogen bonding occurs, because these arrangements are most important to the behavior of dimers and small clusters. As a consequence adjustments are needed for these models to work well in condensed-phase simulations where unfavorable molecular interactions are unavoidable. Unless the *ab initio* based potentials are fit using unfavorable as well as favorable configurations, simulation of bulk-phase systems might require the addition of artificial or empirical repulsive terms. Unfortunately this measure defeats the purpose of using *ab initio* potentials. Nevertheless it is worthwhile to consider the effects of such a modification, to better understand the origins of failure of fitted *ab initio* techniques.

In this work we examine two recently proposed *ab initio*-based pair potentials for HF,[7,10] and we examine the structure, density, and vapor–liquid coexistence properties obtained with them via molecular simulation. For one of the models we further consider a systematic examination of the effect of several features that are or might be neglected in its development or application. The effects are those summarized above, namely three-body contributions to the potential, long-range electrostatic contributions, and modification of short-range repulsive energies.

The article proceeds in Sec. II with a brief description of the *ab initio* based potential models used in this study: that due to Klopper *et al.*[10] (SO-3), and that of Sum, Sandler, and Naicker (SSN).[7] In this section we also discuss the modification we consider in conjunction with the SO-3 model. Section III provides simulation details. In Sec. IV, the simulation results are presented and discussed. Finally, conclusions are made in Sec. V.

II. MODELS

A. Energy surfaces

1. SO-3 model

Klopper *et al.*[10] presented an empirically refined HF potential model formulated using high-level *ab initio* calculations and experimental spectroscopic properties. The investigators gained from previous experience in fitting potential models for HF to *ab initio* surfaces.[24] The advent and availability of higher level treatments allowed for improvement on earlier analytical surfaces. They applied second-order Møller–Plesset (MP2) and explicitly correlated second-order Møller–Plesset (MP2-R12) theory to create a scanned surface of the HF monomer and dimer. Specifically, the scan of the pair potential consisted of 3284 selected points at the described levels of theory with account for monomer stretching. Angular grids were set up at intervals of 20° (for R_{FF} equal to $5.15625\,a_0$), 30° (for R_{FF} equal to 4.875, 5.125, 5.15625, and $5.21875\,a_0$) and 45° (for R_{FF} equal to 4.0, 4.5,

4.75, 5.0, 5.1875, 5.25, 5.5, 6.0, 7.0, and $9.0\,a_0$). For the scan, the basis set consisted of a combination of aug-cc-pVTZ and aug-cc-pVQZ types (a total of 152 basis functions). In addition to the scanned surfaces, minimum energy calculations were performed with explicitly correlated singles and doubles coupled-cluster single double triple calculations including a perturbative correction for triples excitations (CCSD(T)-R12 method). For the minimum calculations, a basis set was constructed by combining aug-cc-pVQZ and aug-cc-pV5Z resulting in 276 basis functions. Through empirical refinements (specifically to capture spectroscopic dissociation energy D_0), the results of the Klopper *et al.*'s work were two potential models, dubbed SO-3 and SC-2.9, that capture a variety of monomer (experimental bond length and HF stretching fundamental ν_{HF}) and dimer properties (electronic binding energies, ground state tunneling splitting, among other properties) agree well in comparison to experiment. They used in fitting the *ab initio* calculations 67 and 61 parameters for SC-2.9 and SO-3, respectively. The functional forms of the potential include effects of repulsion, dispersion and electrostatics (dipole and quadrupole interactions), atom–atom interactions, and terms for angular variations of a dimer surface. The model has been compared in an *ab initio* study by Tschumper *et al.*[25,26] to find significant agreement for the analyzed dimer properties.

2. SSN model

Sum *et al.*[7] developed an HF model (referred to here as SSN) that is fit to *ab initio* calculations based symmetry-adapted perturbation theory, and they further applied it to vapor–liquid equilibrium (VLE) calculations. In this work we reproduce those VLE calculations, and examine also the structural properties of the model as given by the radial distribution function (RDF).

Briefly, the methodology was equivalent to fourth-order Møller–Plesset (MP4) theory. The basis set consisted of 6s3p2d1f orbitals for the fluorine and 3s2p1d orbitals for the hydrogen. Additional bond functions of 3s2p1d were placed midway between the center of mass of the pair of molecules. To amass energetic information, a scan of 529 configurations over F–F radial distances of 2.0, 2.5, 3.0, 3.5, 4.0, 5.0, and 6.0 Å and corresponding angular grids was performed. Further calculations were performed to explore the minimum energy region. The potential model is of the form

$$E_{AB}^{\mathrm{int}}=\sum_{a\ \mathrm{in}\ A}\sum_{b\ \mathrm{in}\ B}\left[\left(\frac{1}{r_{ab}}+A_{ab}\right)\exp(\alpha_{ab}-\beta_{ab}r_{ab})+f_1(\delta_1^{ab}r_{ab})\frac{q_aq_b}{r_{ab}}-\sum_{n=6,8,10}f_n(\delta_n^{ab}r_{ab})\frac{C_n^{ab}}{r_n^{ab}}\right], \quad (1)$$

$$f_n(x)=1-\exp(-x)\sum_{k=0}^{n}\frac{x^k}{k!}, \quad (2)$$

where r_{ab} designates the distance between sites and charges, q_a, on particular molecules. The site–site parameters consisted of α_{ab}, β_{ab}, A_{ab}, C_n^{ab}, and δ_n^{ab} fit to the *ab initio* calculated energies. The bond length of HF was set to the Huber and Herzberg[27] value, 0.91681 Å. Charges for the model were developed from MP3 calculations with single-molecule basis sets that yielded a dipole moment of 1.85 D. An off atom site for HF was placed 0.426 190 Å from the fluorine atom. Sum *et al.* present a complete description elsewhere.[6,7]

B. Modifications to the SO-3 surface

In this work we examine the SO-3 surface in its original form, and also consider several modifications or options for its implementation and examine their effect on the computed properties.

1. Intramolecular refinement

The intramolecular stretching effect in the condensed phase can be significant for HF (as observed in our simulations). To limit the extent that the molecule would stretch, the molecule was constrained while keeping the essential features of the potential (features remain consistent within ± 0.04 Å of the equilibrium length). The reason for such an alteration is to avoid any unrealistic overstretching in liquid-phase simulations without damaging the energetics of the monomer equilibrium structure. The stretching potential defined by the SO-3 model in Klopper *et al.*[10] is

$$V_G(r)=\exp(-2ar)\left(\frac{B}{(1-b^2\exp(-2ar))^2}-\frac{A}{(1+b^2\exp(-2ar))^2}\right), \quad (3)$$

with $a=0.5847305$, $b=1.28$, $A/h=953320.3\ \mathrm{cm}^{-1}$, and $B/h=164\,766.75\ \mathrm{cm}^{-1}$ (h is Planck's constant). In this work we modified it as follows:

$$V_G^{\mathrm{mod}}(r)=V_G(r)+(V_G(r)/1.25)^8. \quad (4)$$

This intramolecular H–F potential was used in all calculations here.

2. Atom-core repulsion

The development of the SO-3 potential surface paid great attention to areas of hydrogen bonding, because of its aim to describe experimental properties of spectroscopic importance. It is understandable then that the unfavorable energetic region would be analyzed less thoroughly than the regions in the vicinity of the minimum energy configuration. Specifically for the SO-3 surface the scan in repulsive regions, for F–F distances (R_{FF}) less than $4.875\,a_0$, used a coarse angular grid of 45° with a radial (varying R_{FF}) grid at 4.0, 4.5, and $4.75\,a_0$. In addition a technique was used to discount unfavorable regions through probes based on another analytical potential (dubbed SQSBDE).[28] To investigate effects due to such regions, we added terms in the potential to act much like a soft repulsive sphere, using the Born–Mayer form

$$U_{ij}=A_{ij}\exp(-B_{ij}r_{ij}), \quad (5)$$

with i and j referring to atoms on different molecules separated by distance r_{ij}. Here $A_{ij}=10^{10}$ kcal/mol for all inter-

actions. Three different interactions, H–F, H–H, and F–F required three different parameters for B, 19.0, 9.7, and 9.0 Å, respectively. The effect on the hydrogen-bonding region remains quite small while it significantly buttresses the repulsive core. The repulsion is rather extreme but short ranged; a more realistic value of A_{ij} for core repulsions is significantly lower. The aim in using such a hard repulsion is to gauge its effect on the properties, more than attempting to produce a good match with experiment.

3. Three-body surface

The importance of multibody effects in HF has been well documented.[14,25,29] One approach to incorporating multibody effects employs polarizable models, applying electrostatic features on the molecule and permitting them to morph in response to the electric field originating from the molecules in its vicinity. This is perhaps the most popular method in current use for introducing multibody effects. In keeping with the theme of *ab initio* derived potential models, we consider instead a 12-dimensional analytical three-body surface that has been fit to the of three-body energetics of HF. This model, HF3BG, was tested by its developers[14] on clusters of up to eight HF molecules with adequate success in capturing spectroscopic properties. Further analysis in comparison to *ab initio* calculations was performed by Tschumper *et al.*[25] The model was derived from second-order Møller–Plesset (MP2) calculations with counterpoise correction at a basis set level of double-zeta polarization. The HF3BG model was fit primarily to induction terms arising due to dipole moments for three molecules. Additionally, simple short range functions were used to enhance the potential model. Classical and quantum sampling techniques were used to select 3000 configurations of HF trimer. Since 12 dimensions are being scanned, Quack *et al.*[14] used an elaborate sampling scheme to arrive at energy values of the $(HF)_3$ surface. Complete enhancements and refinements to the surface are described fully by Quack *et al.*[14]

Implementation of the model into simulation was straightforward. The potential is applied to all triplets that can be formed from the molecules in the simulation volume. As with the two-body surface, a radial cutoff was imposed at 9 Å, such that the potential is set to zero if any molecule in the triplet is more than 9 Å distant from another (as measured by the F atom positions).

4. Ewald summation

It is not unusual in condensed-phase calculations to neglect contributions from the long-range electrostatics. This is particularly understandable with the fitted *ab initio* surfaces, where it can be difficult to identify the electrostatic origins of the complex functional forms used for the fitting. The accounting for dipole long-range interactions in fluid phases can be accomplished by applying an Ewald summation. Other higher order terms due to quadrupole moments and electrostatic fields do arise in this potential model. For the purpose of the present analysis, higher order terms are assumed to be less important than the dipole–dipole interaction so their long-range interactions are not considered.

Heyes *et al.*[19] mapped out the terms that contribute to the energy due to the periodic arrangement of dipole moments. The total Ewald contribution is as follows:

$$\Phi=\frac{1}{2}\sum_{i=1}^{N}\sum_{j=1}^{N}\sum_{n'}^{\infty}[(\mu_i\cdot\mu_j)B(r_{nij})-(\mu_i\cdot r_{nij})(\mu_j\cdot r_{nij})\times C(r_{nij})]+\frac{2\pi}{V}\sum_{h\neq 0}^{\infty}h^{-2}\exp\left(\frac{-h^2}{4\kappa^2}\right)\times\left\|\sum_{i=1}^{N}\mu_i\cdot h\exp(ih\cdot r_i)\right\|^2-\sum_{i=1}^{N}\frac{2\kappa^3\mu_i^2}{3\pi^{1/2}}, \tag{6a}$$

$$\Phi=\Phi^r+\Phi^k+\Phi^s, \tag{6b}$$

where $h/2\pi$ is summed over all cubic lattice vectors, and

$$B(r)=\operatorname{erfc}(\kappa r)r^{-3}+2\kappa\pi^{-1/2}\exp(-\kappa^2r^2)r^{-2}, \tag{7}$$

$$C(r)=3\operatorname{erfc}(\kappa r)r^{-5}+2\kappa\pi^{-1/2}(2\kappa^2+3r^{-2})\times\exp(-\kappa^2r^2)r^{-2}. \tag{8}$$

The term κ is set to $5/L$ for all state conditions, where L is the edge length of the simulation volume. The dipole moment, μ_i, is described in the SO-3 potential by a term related to the monomer length[10]

$$\mu_i=\mu_e+\mu_e'\eta_i a_0, \tag{9}$$

$$\eta_i=\tanh(r_i/a_o-r_e/a_o), \tag{10}$$

with μ_e/ea_0 equal to 0.707 r_e/a_o equal to 1.7327, and μ_e' calculated via a finite difference method.

In order to apply the Ewald summation theory conveniently to the SO-3 model, some modifications were employed. The real-space surface of Eq. (6a) was first broken into two ranges of interactions as below:

$$\Phi^r=\frac{1}{2}\sum_{i=1}^{N}\sum_{j=1}^{N}\sum_{n'}^{\infty}(\mu_i\cdot\mu_j)-(\mu_i\cdot r_{nij})(\mu_j\cdot r_{nij})-\frac{1}{2}\sum_{i=1}^{N}\sum_{j=1}^{N}\sum_{n'}^{\infty}(\mu_i\cdot\mu_j)D(r_{nij})-(\mu_i\cdot r_{nij})\times(\mu_j\cdot r_{nij})E(r_{nij}), \tag{11}$$

$$D(r)=\operatorname{erf}(\kappa r)r^{-3}+2\kappa\pi^{-1/2}\exp(-\kappa^2r^2)r^{-2}, \tag{12}$$

$$E(r)=3\operatorname{erf}(\kappa r)r^{-5}+2\kappa\pi^{-1/2}(2\kappa^2+3r^{-2})\times\exp(-\kappa^2r^2)r^{-2}, \tag{13}$$

We replace the first term, on the right-hand side of Eq. (11) with

$$\Phi^r=\frac{1}{2}\sum_{i=1}^{N}\sum_{j=1}^{N}\mu_i\mu_j(r_{ij}^3+c_s)^{-1}\left(-\cos\theta_i\cos\theta_j+\frac{1}{2}\sin\theta_i\sin\theta_j\cos\tau\right)+\cdots \tag{14}$$

as given by Klopper *et al.*

III. SIMULATION DETAILS

We performed simulation of model HF using the SO-3 potential and variations on it, as well as the SSN model. We

examined a variety of properties requiring different simulation methods. First we examined all interatomic RDFs by simulation in the canonical (NVT) ensemble, for temperatures and densities set to experimental values given by Pfleiderer *et al.*[30] Second, isothermal isobaric (NPT) simulations were performed to calculate densities at corresponding experimental pressures and temperatures. Finally Gibbs ensemble calculations[17,31] were conducted to measure all VLE properties.

All simulations consisted of the same simulation length [5×10^4 cycles, a cycle being one Monte Carlo (MC) trial per molecule] and number of molecules (500). Simulations started from equilibrated configurations. Appropriate simulation moves were employed for each ensemble. NVT simulations consisted of displacement and rotation moves. The NPT ensemble used volume moves in addition to displacement and rotation. Finally Gibbs ensemble added particle exchange moves to displacement, rotation and volume-exchange moves. Step sizes were adjusted to obtain a 40% acceptance rate of each trial. Vapor pressures were sampled in the Gibbs ensemble through a method of measuring fluctuations in volume.[32]

The availability of HF experimental RDFs[30] for a range of temperatures and pressures allows us to compare NVT simulation results to the structural properties. Simulation values can be compared by measuring RDFs for each combination of atoms and comparing them to experiment, for which the following blend of RDFs has been measured:

$$g(r)=0.4966g_{\mathrm{DF}}+0.2104g_{\mathrm{FF}}+0.2930g_{\mathrm{DD}}. \tag{15}$$

Our NVT ensemble simulations were conducted to match conditions of temperature and density for which experimental data[30] are available: 300 K and 2 bar, which is a liquid; and 473 K and 78 bar, which is supercritical. The NPT ensemble simulations were performed at these conditions also, to examine the correspondence between the densities of the models versus experiment.

VLE properties were calculated over a range of temperatures, via Gibbs ensemble simulation, starting from 225 K and moving toward the critical point. Vapor pressures, coexistence densities, and heat of vaporizations were collected.

IV. RESULTS AND DISCUSSION

Results for the structural properties of the HF model fluids are presented in Figs. 1 and 2. Corresponding experimental data are presented there also.[30] It is clear that both the SO-3 and the SSN models fail to capture the liquid structure. The first peak in the RDF, formed mainly from the g_{HF} contribution, is significantly underestimated, and shifted to greater separation, indicating too-weak cohesion in the models. In contrast, the region at about 3 Å, corresponding to the first shell of F–F separation, is much too large. Densities computed by separate NPT simulations at the experimental state conditions are shown in Table I. The simulation densities overestimate the true densities for the liquid state (corresponding to Fig. 1) and underestimate it for the supercritical state (corresponding to Fig. 2) (again, the RDFs are measured in NVT simulations at the experimental densities). Addition of the repulsive core is capable of bringing the liquid density into agreement with experiment (it is fit to do this), but unsurprisingly it has no effect on the supercritical-fluid density. None of the modifications improve this density significantly. To ensure that the low density does not result from inadequacies in the MC sampling of configurations, we also performed some simulations using an association-bias method,[33] but observed no change in the results.

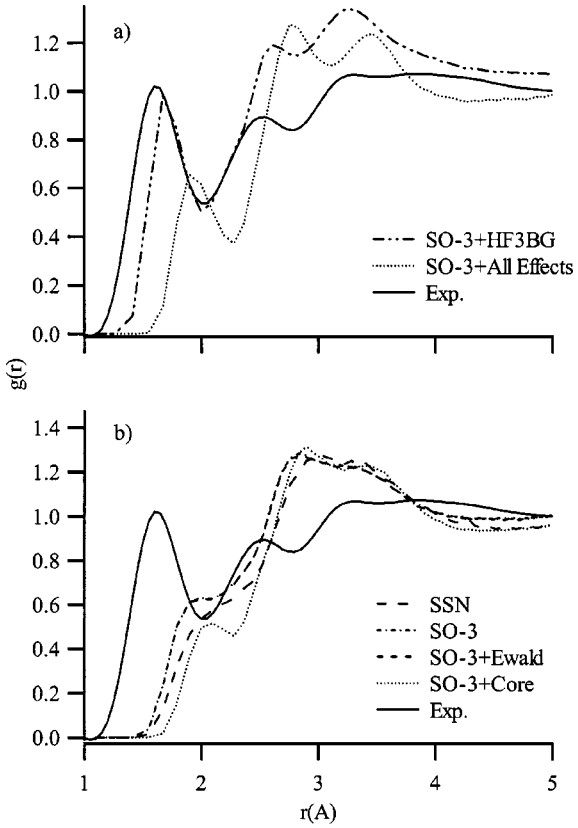

FIG. 1. Radial distribution functions for HF at 300 K and 2 bar. Model results are from simulations conducted at the density of the experimental measurements. Experimental data are from Pfleiderer *et al.* (Ref. 30) Curves represent a combination of three atom–atom radial distributions according to Eq. (15) to produce $g(r)$. Top graph (a) shows RDFs with three-body contributions. Bottom graph (b) shows pair potentials.

In Figs. 3 and 4, the VLE densities are given for the two HF pair potentials, again compared to experiment.[34–38] Underestimation of the critical point can be clearly seen, along with exaggerated liquid densities at low temperatures. The overestimation of liquid densities seems to be a universal characteristic of *ab initio* pair potential models for HF.[7,39] Vapor pressures are shown in Fig. 5, and exhibit a consistent overestimation of the experimental vapor pressure[34–36] at all temperatures, again indicating a lack of sufficient cohesion. Figure 6 shows another typical characteristic of HF potential models. The heat of vaporization is grossly misrepresented in comparison to experimental behavior[34,35,40] with temperature, which displays (atypically) a maximum.

We now consider how variations on the SO-3 model implementation influence these results. Modifications consider inclusion of the Ewald sum for the long range dipole–dipole interactions, a semiempirical form that modifies SO-3 by bolstering the short-range repulsion, and addition of the HF3BG three-body potential. We consider the effect of each of these modifications separately, and then the effect of ap-

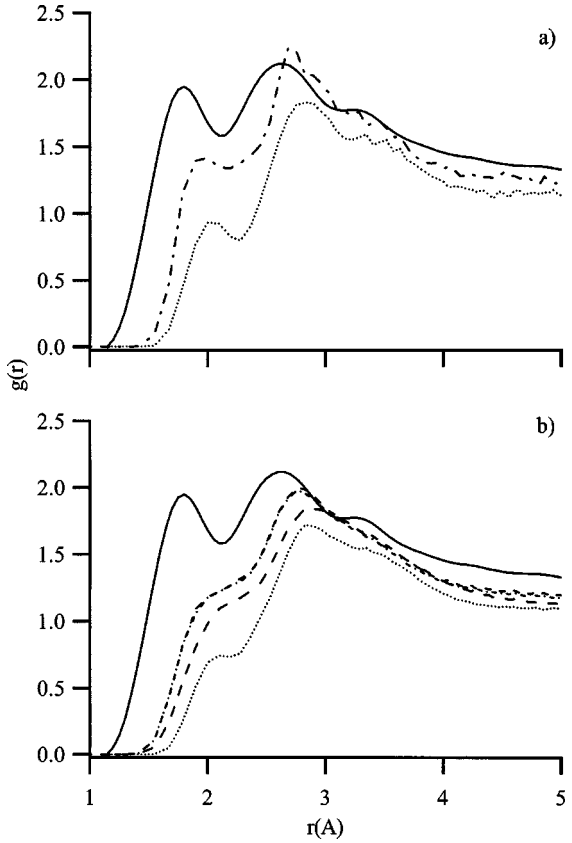

FIG. 2. Same as Fig. 1, but at 473 K and 78 bar.

plying them all together. Results from simulations using these modifications are included in Figs. 1–6.

Inclusion of Ewald-sum long-range electrostatic interactions does little to change the calculated RDFs and densities. If anything it tends to further wash out the F–H peak, and it has almost no effect on the coexistence behavior—densities, vapor pressure, or heat of vaporization. This is perhaps an indicator that the important effects are occurring at short ranges of separation.

The semiempirical repulsion enhancement improves the short-range structural features of the RDF, but not as much as one might expect. There is a slight sharpening of the first peak, and little effect beyond that. The coexistence properties, however, are markedly improved, which is not surprising given that the experimental liquid densities were used to adjust the potential. But at the same time it significantly lowers the critical point and further raises the vapor pressure, such that the overall comparison with experiment is hardly an improvement. Coincidently, the coexistence curve of the repulsion-enhanced potential exhibits properties (coexistence densities, vapor pressures, and heat effects) similar to those seen with the SSN energy surface.

TABLE I. Densities of HF (g/cm^3) from NPT MC simulation and experiment.[a] Numbers in parentheses indicate the 67% confidence limit for the last digit of the value.

	300 K, 2 bar	473 K, 78 bar
SSN	0.977(9)	0.0531(1)
SO-3	1.191(1)	0.0557(2)
SO-3+Ewald	1.207(5)	0.0556(3)
SO-3+core	0.962(3)	0.0493(1)
SO-3+HF3BG	1.343(9)	0.0658(3)
SO-3+all effects	1.040(4)	0.0506(2)
Experiment	0.962	0.236

[a]See Refs. 15, 30, 37, and 41.

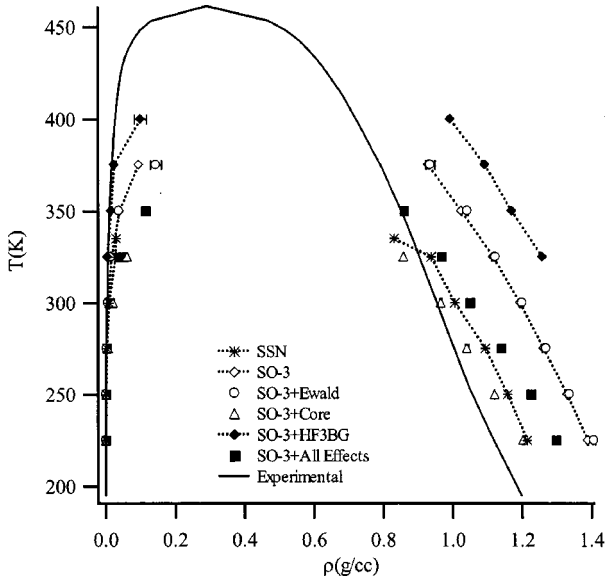

FIG. 3. Vapor–liquid equilibrium densities as calculated from the HF potential models (via Gibbs ensemble MC simulation). Experimental critical point (Ref. 34) is 0.290 g/cm^3 and 461 K. Solid line describes experimental data (Refs. 34–38). Dotted lines correspond to potential models given in literature (Refs. 7, 10, and 14). Solid markers correspond to potentials that include three-body interactions. Open markers represent pair potential models. Error bars are shown only when larger than the symbol size.

Now we turn to consider the effects of incorporating the explicit three-body interactions, which should provide some indication of the need for introducing multibody effects to the *ab initio* potential model. The potential is defined to include the SO-3 surface plus the HF3BG surface. Separately

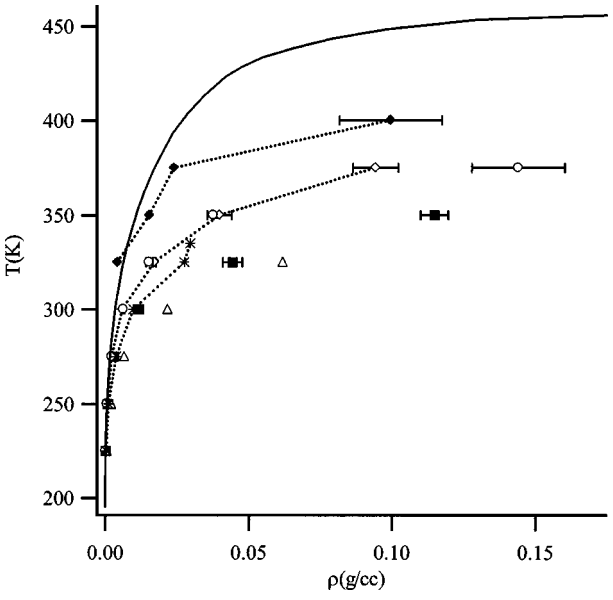

FIG. 4. Expanded view of vapor-phase coexistence densities from Fig. 3.

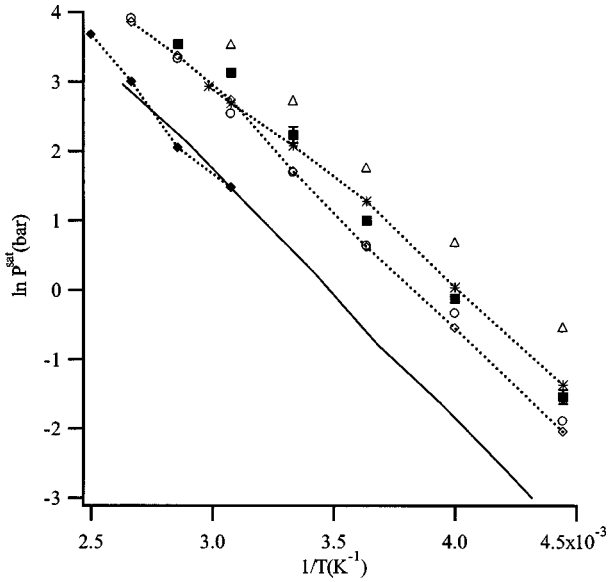

FIG. 5. Clausius–Clapeyron plot of saturated vapor pressures. Symbols as in Fig. 3. Experimental data are from Refs. 34–36.

we consider this SO-3+HF3BG with Ewald long-range dipole interactions and the enhanced repulsion, thus including all modifications.

In examining the structure for the three-body potentials, we see prominent peaks that bring them a good bit closer to agreement with experiment, particularly for the liquid-density system. This is seen especially for the case where three-body effects are added alone. However, this same modification causes a substantial worsening of the already bad characterization of the liquid phase coexistence density, an improvement in the critical temperature, and very good agreement for the vapor pressure. Then upon addition of the other modifications, many of these changes are nullified, and all behaviors trend back toward that for the repulsion-enhanced potential without three-body contributions. No real improvement in heat of vaporization is seen in either three-body modification.

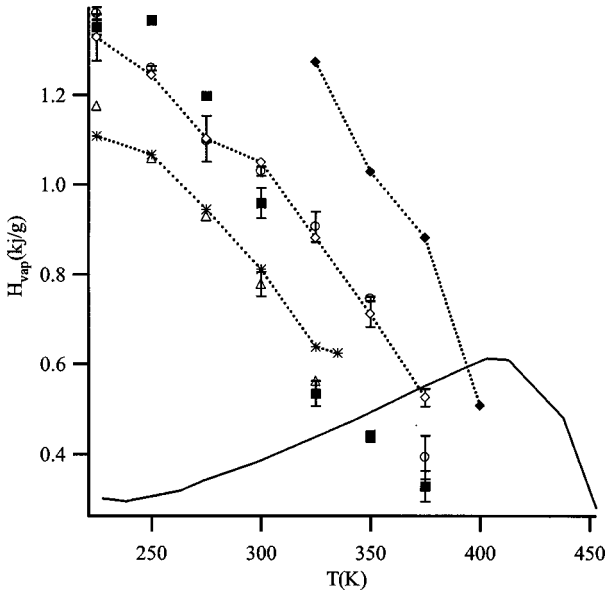

FIG. 6. Heat of vaporization. Symbols as in Fig. 3. Experimental data are from Refs. 34, 35, and 40.

Let us summarize the observations and try to draw some conclusions from them. First, there is not enough cohesion acting in any of the two-body potentials—the hydrogen bonding is not sufficiently in play to produce some important features. This is evidenced by the attenuated H–F peak in the RDF, the low supercritical-vapor density, the low critical temperature, the high vapor pressure, and the failure of the heat of vaporization to exhibit a peak indicative of vapor-phase clustering. Addition of three-body effects greatly improves this situation, sharpening the H–F peak in the RDF and giving rise to much better vapor pressures. The cost of this improvement is substantial worsening of the liquid-phase density (cf. Fig. 3 and Table I), which was already pretty bad; moreover the three-body contribution provides only a tiny improvement in the supercritical-fluid densities.

The lack of cohesion in the models is, paradoxically, accompanied by a lack of sufficient repulsion: the F–F peak in the RDF is too large, as are the liquid-phase densities. But the supercritical-fluid densities are too low for both the two-body potentials and the three-body modifications (which the liquid indicates is adding substantial cohesion). We surmise that the supercritical density is low because these low-density molecules cannot get close enough to the hydrogen bond—i.e., the repulsion is not too weak, but too strong. Thus when the core contribution is bolstered, we find that (even though this added repulsion is short ranged) the cohesive influence is severely diminished: witness the greatly attenuated H–F peak in the liquid RDF, the slight increase in the vapor pressure, and lowering of the critical temperature, and the decrease in the supercritical-fluid density (Table I). Incidentally, the SSN model seems to end up striking the same balance as SO-3+core.

Thus the general picture indicates that the cohesive hydrogen bonds and the repulsive core are delicately balanced, and relatively small changes can push the behavior disproportionately towards one or the other. One should recall that the development of these models emphasized the hydrogen-bonded configurations, so it is likely that the lack of cohesion is due not to deficiencies in the attractive components, but to inadequate characterization of the repulsive, nonassociated interactions. We think that the direction for improvement is to soften the core while perhaps enlarging it. A larger, softer core would push molecules away from each other if they are nonspecifically associated, while promoting their ability to form hydrogen-bonding associations when properly oriented. In this way all phases can gain cohesion at the same time that the liquid is being expanded. Alternatively (or in addition), the expansion of the liquid might be facilitated by promoting specific association, with the idea that the resulting order of the liquid-phase structures would promote lower density (akin to the well known effect in water, where ordering leads to a lowering of density).

At this point we risk overspeculating about the behavior of what is inarguably a complex dependency on some carefully balanced forces. We think that further progress in this modeling effort requires examination of potential-energy sur-

faces, and exploration of some alternative modeling methods. Three-body effects are significant, but can yield improvement only when built on a good two-body potential surface. Efforts to formulate a better pair potential must consider all orientations of two molecules, with special attention given to F–F separations in the range of 2.2–2.6 Å, as this is where the balance between the (repulsive) two-body and (attractive) three-body contributions is most delicate.

V. CONCLUSION

This work compares two *ab initio* based pair potentials for HF, and considers for one of them the modifications that should make it perform better for the liquid phase. These modifications introduce long-range electrostatic interactions, short-range repulsion, and three-body effects, respectively. We examined structural properties and densities for two different states. Further we examine VLE properties including heats of vaporization, vapor pressures, and coexistence densities. The inclusion of long-range electrostatic interactions does little to change the calculated properties. The inclusion of repulsive terms improves the behavior of the density (as designed), but reduces performance in predicting other properties. The inclusion of three-body effects markedly improves the structure, but still does not bring it into agreement with experiment, and it brings mixed results in improving other properties. Inclusion of all effects does not yield qualitatively better performance than any of the other variations.

On the positive side, this work shows that inclusion of three-body interactions can have significant, favorable impact on liquid phase structure, although effects on thermophysical properties are mixed. We remain hopeful that, at least in the modeling of HF and perhaps other hydrogen-bonding systems, incorporation of three-body effects with more robust pair potentials can lead to improvements in a broad range of properties for both liquid and vapor phases. We think that to achieve this, fitting of the *ab initio* derived surface must consider unfavorable configurations and focus a bit less on minimum-energy configurations.

ACKNOWLEDGMENTS

We are grateful for several contributions to our work. Financial support was provided by the National Science Foundation, Grant No. CTS-0076515. Computing facilities were provided by the University at Buffalo Center for Computational Research. We thank Amadeu Sum for providing us with the source code for the SSN *ab initio* potential. We thank Martin Suhm for providing source code for dimer and trimer potentials (located at http://www-suhm.uni-pc.gwdg.de/suhmpubs.htm). Finally Pal Jedlovszky graciously provided us with Pfleiderer's experimental RDF data.

[1] J. I. Siepmann, NIST Spec. Publ. **975**, 110 (2001).
[2] R. Car and M. Parrinello, Phys. Rev. Lett. **55**, 2471 (1985).
[3] B. Chen, I. Ivanov, and M. L. Klein, Abstr. Pap. - Am. Chem. Soc. **224**, U505 (2002); S. Izvekov and G. A. Voth, J. Chem. Phys. **116**, 10372 (2002); A. J. Sillanpaa, C. Simon, M. L. Klein, and K. Laasonen, J. Phys. Chem. B **106**, 11315 (2002).
[4] M. Kreitmeir, H. Bertagnolli, J. J. Mortensen, and M. Parrinello, J. Chem. Phys. **118**, 3639 (2003).
[5] A. K. Sum and S. I. Sandler, Fluid Phase Equilibria, **160**, 375 (1999); A. K. Sum and S. I. Sandler, Ind. Eng. Chem. Res. **38**, 2849 (1999); A. K. Sum, S. I. Sandler, R. Bukowski, and K. Szalewicz, J. Chem. Phys. **116**, 7627 (2002); **116**, 7637 (2002).
[6] A. K. Sum and S. I. Sandler, Mol. Phys. **100**, 2433 (2002).
[7] A. K. Sum, S. I. Sandler, and P. K. Naicker, Fluid Phase Equilibria **199**, 5 (2002).
[8] A. D. Mackie, J. Hernandez-Cobos, and L. F. Vega, J. Chem. Phys. **111**, 2103 (1999); K. Honda, *ibid.* **117**, 3558 (2002).
[9] E. M. Mas, R. Bukowski, and K. Szalewicz, J. Chem. Phys. **118**, 4404 (2003).
[10] W. Klopper, M. Quack, and M. A. Suhm, J. Chem. Phys. **108**, 10096 (1998).
[11] D. P. Visco and D. A. Kofke, J. Chem. Phys. **109**, 4015 (1998).
[12] A. E. Barton and B. J. Howard, Faraday Discuss. Chem. Soc. **73**, 45 (1982).
[13] E. Clementi and G. Corongiu, Int. J. Quantum Chem. **10**, 31 (1983); J. D. G. Corongiu and E. Clementi, *ibid.* **18**, 701 (1984).
[14] M. Quack, J. Stohner, and M. A. Suhm, J. Mol. Spectrosc. **599**, 381 (2001).
[15] P. Jedlovszky, M. Mezei, and R. Vallauri, J. Chem. Phys. **115**, 9883 (2001).
[16] P. Jedlovszky and R. Vallauri, J. Chem. Phys. **107**, 10166 (1997).
[17] D. Frenkel and B. Smit, *Understanding Molecular Simulation: From Algorithms to Applications* (Academic, New York, 1996).
[18] M. P. Allen and D. J. Tildesley, *Computer Simulation of Liquids* (Clarendon, Oxford, 1987).
[19] D. M. Heyes, Phys. Rev. B **49**, 755 (1994).
[20] T. M. Nymand and P. Linse, J. Chem. Phys. **112**, 6152 (2000); **112**, 6386 (2000); T. M. Nymand, P. Linse, and P. O. Astrand, Mol. Phys. **99**, 335 (2001).
[21] I. Nezbeda and J. Kolafa, Mol. Phys. **97**, 1105 (1999); I. Nezbeda and M. Lisal, *ibid.* **99**, 291 (2001); I. Nezbeda and U. Weingerl, *ibid.* **99**, 1595 (2001).
[22] P. Jedlovszky and R. Vallauri, Mol. Phys. **92**, 331 (1997); R. G. Della Valle and D. Gazzillo, Phys. Rev. B **59**, 13699 (1999).
[23] M. L. Klein, I. R. Mcdonald, and S. F. Oshea, J. Chem. Phys. **69**, 63 (1978).
[24] M. Quack and M. A. Suhm, in *Conceptual Perspectives in Quantum Chemistry*, edited by J.-L. Calais and E. S. Kryachko (Kluwer, Dordrecht, 1997), Vol. III, p. 415.
[25] G. S. Tschumper, Y. Yamaguchi, and H. F. Schaefer, J. Chem. Phys. **106**, 9627 (1997).
[26] G. S. Tschumper, M. D. Kelty, and H. F. Schaefer, Mol. Phys. **96**, 493 (1999).
[27] K. P. Huber and G. Herzberg, *Molecular Spectra and Molecular Structure, 4: Constants of Diatomic Molecules*, Van Nostrand Reinhold, New York (1979).
[28] M. Quack and M. A. Suhm, J. Chem. Phys. **95**, 28 (1991).
[29] M. M. Szczesniak and G. Chalasinski, THEOCHEM **93**, 37 (1992); M. P. Hodges, A. J. Stone, and E. C. Lago, J. Phys. Chem. A **102**, 2455 (1998); G. Chalasinski, S. M. Cybulski, M. M. Szczesniak, and S. Scheiner, J. Chem. Phys. **91**, 7048 (1989).
[30] T. Pfleiderer, I. Waldner, H. Bertagnolli, K. Todheide, and H. E. Fischer, J. Chem. Phys. **113**, 3690 (2000).
[31] A. Z. Panagiotopoulos, Mol. Phys. **61**, 813 (1987).
[32] V. I. Harismiadis, J. Vorholz, and A. Z. Panagiotopoulos, J. Chem. Phys. **105**, 8469 (1996).
[33] S. Wierzchowski and D. A. Kofke, J. Chem. Phys. **114**, 8752 (2001); B. Chen and J. I. Siepmann, J. Phys. Chem. B **104**, 8725 (2000).
[34] C. P. C. Kao, M. E. Paulaitis, G. A. Sweany, and M. Yokozeki, Fluid Phase Equilibria. **108**, 27 (1995).
[35] K. Fredenhagen, Z. Anorg. Allg. Chem. **210**, 210 (1933).
[36] C. E. Vanderzee and W. W. Rodenburg, J. Chem. Thermodyn. **2**, 461 (1970).
[37] E. U. Franck and W. Spalthoff, Z. Elektrochem. **61**, 348 (1957).
[38] J. H. Simons and J. W. Bouknight, J. Am. Chem. Soc. **54**, 129 (1932).
[39] D. P. Visco and D. A. Kofke, Fluid Phase Equilibria **160**, 37 (1999).
[40] R. M. Yabroff, J. C. Smith, and E. H. Lightcap, J. Chem. Eng. Data **9**, 178 (1964).
[41] E. U. Franck, G. Wiegand, and R. Gerhardt, J. Supercrit. Fluids **15**, 127 (1999).